01 Apr 2017

Inelastic Rate Coefficients for Collisions of C_6H^- with H_2 and He

Kyle M. Walker

François Lique

Fabien Dumouchel

Richard Dawes
Missouri University of Science and Technology, dawesr@mst.edu

Recommended Citation

K. M. Walker et al., "Inelastic Rate Coefficients for Collisions of C_6H^- with H_2 and He," *Monthly Notices of the Royal Astronomical Society*, vol. 466, no. 1, pp. 831-837, Oxford University Press, Apr 2017.
The definitive version is available at https://doi.org/10.1093/mnras/stw3065

Monthly Notices
of the
ROYAL ASTRONOMICAL SOCIETY

MNRAS **466,** 831–837 (2017)
Advance Access publication 2016 November 29

doi:10.1093/mnras/stw3065

Inelastic rate coefficients for collisions of C_6H^- with H_2 and He

Kyle M. Walker,[1⋆] François Lique,[1⋆] Fabien Dumouchel[1] and Richard Dawes[2]

[1]*LOMC – UMR 6294, CNRS – Université du Havre, 25 rue Philippe Lebon, BP 1123, F-76063 Le Havre cedex, France*
[2]*Department of Chemistry, Missouri University of Science and Technology, Rolla, MO 65409, USA*

Accepted 2016 November 22. Received 2016 November 21; in original form 2016 October 14

ABSTRACT

The recent detection of anions in the interstellar medium has shown that they exist in a variety of astrophysical environments – circumstellar envelopes, cold dense molecular clouds and star-forming regions. Both radiative and collisional processes contribute to molecular excitation and de-excitation in these regions so that the 'local thermodynamic equilibrium' approximation, where collisions cause the gas to behave thermally, is not generally valid. Therefore, along with radiative coefficients, collisional excitation rate coefficients are needed to accurately model the anionic emission from these environments. We focus on the calculation of state-to-state rate coefficients of the C_6H^- molecule in its ground vibrational state in collisions with para-H_2, ortho-H_2 and He using new potential energy surfaces. Dynamical calculations for the pure rotational excitation of C_6H^- were performed for the first 11 rotational levels (up to $j_1 = 10$) using the close-coupling method, while the coupled-states approximation was used to extend the H_2 rate coefficients to $j_1 = 30$, where j_1 is the angular momentum quantum number of C_6H^-. State-to-state rate coefficients were obtained for temperatures ranging from 2 to 100 K. The rate coefficients for H_2 collisions for $\Delta j_1 = -1$ transitions are of the order of 10^{-10} cm^3 s^{-1}, a factor of 2 to 3 greater than those of He. Propensity rules are discussed. The collisional excitation rate coefficients produced here impact astrophysical modelling since they are required for obtaining accurate C_6H^- level populations and line emission for regions that contain anions.

Key words: molecular data – molecular processes – scattering – ISM: molecules.

1 INTRODUCTION

Anions have been long thought to reside in the interstellar medium (ISM; Dalgarno & McCray 1973; Herbst 1981). However, due to the lack of fundamental laboratory data and their relatively low abundance with respect to the neutral molecules, their detection has occurred only within the last decade. The first detected anion, C_6H^-, was observed in the circumstellar envelope of the evolved star IRC +10216 and in the cold molecular cloud TMC-1 (McCarthy et al. 2006). C_6H^- has since been found in other star-forming regions, such as in the dark clouds L1527 (Sakai et al. 2007), L1544 and L1521F (Gupta et al. 2009). Five other anions have also been detected since then, including C_4H^- (Cernicharo et al. 2007), C_8H^- (Brünken et al. 2007), C_3N^- (Thaddeus et al. 2008), C_5N^- (Cernicharo et al. 2008) and CN^- (Agúndez et al. 2010), all in the original sources IRC +10216 and TMC-1.

These cool, low-density regions are prime sites for studying anions in the ISM. Anions affect the rates of cloud collapse and star formation by lowering the free electron density, and their abundances help constrain the chemical network of the ISM. However, current models fail to reproduce detected anion-to-neutral ratios.

The determination of abundances from molecular spectra requires radiative and collisional excitation rate coefficients with the most abundant species, which, in these regions, is molecular hydrogen. In the absence of collisional rate coefficients, the quantum-level populations are usually estimated assuming local thermodynamic equilibrium (LTE) – that the populations are governed by a Boltzmann distribution. However, this is generally not a good approximation in the regions where anions reside. Although the LTE approximation is useful on the surface of stars or other high-density or energetic environments, the cool regions in the ISM contain molecules with level populations that do not behave thermally. Therefore, collisional rate coefficients must be either theoretically calculated or experimentally determined to accurately model these regions.

Kłos & Lique (2011) computed the first and only anion rate coefficients relevant to ISM studies by performing quantum scattering calculations for the rotational excitation of CN^- with H_2. State-to-state rate coefficients for the lowest 11 rotational levels for temperatures from 5 to 100 K were calculated and found to be significantly larger than neutral species such as CO. In light of this, it was concluded that the use of neutral rate coefficients as estimates

⋆ E-mail: kyle.walker@univ-lehavre.fr (KMW); francois.lique@univ-lehavre.fr (FL)

Table 1. C_6H^- rotational energy levels.

j_1	ϵ_{j_1} (cm^{-1})	j_1	ϵ_{j_1} (cm^{-1})
0	0.000	21	21.210
1	0.092	22	23.230
2	0.275	23	25.342
3	0.551	24	27.546
4	0.918	25	29.841
5	1.377	26	32.229
6	1.928	27	34.708
7	2.571	28	37.278
8	3.306	29	39.941
9	4.132	30	42.696
10	5.050	31	45.542
11	6.060	32	48.480
12	7.162	33	51.510
13	8.356	34	54.632
14	9.641	35	57.845
15	11.018	36	61.151
16	12.488	37	64.548
17	14.048	38	68.037
18	15.701	39	71.617
19	17.446	40	75.290
20	19.282	41	79.054

for those of anions would not be accurate for modelling interstellar line emission.

Along with being the first anion detected, C_6H^- is also the most abundant interstellar anion observed. The focus in this paper is to present inelastic rate coefficients for the collisions of C_6H^- with H_2 and He. Fully quantum scattering calculations were carried out on the highvel *ab initio* potential energy surfaces (PESs) of Walker et al. (2016). While Walker et al. (2016) presented preliminary collisional cross-section calculations of these systems, the main focus here is the computation of collisional rate coefficients. The close-coupling (CC) method was used to compute cross-sections, for the first 11 rotational levels of C_6H^-, while the coupled-states (CS) approximation extended the H_2 cross-sections to the first 30 rotational levels. Cross-sections were calculated for collisional energies up to 500 cm^{-1}, and (de-) excitation rate coefficients were obtained for the temperature range of 2–100 K. These scattering calculations will help constrain the physical and chemical conditions in the ISM, especially for astrophysical environments that contain anions such as IRC +10216.

2 SCATTERING CALCULATIONS

We consider collisions of C_6H^- with para-$H_2(j_2 = 0)$ and ortho-$H_2(j_2 = 1)$ described by

$$C_6H^-(j_1) + \text{o-; p-}H_2(j_2) \rightarrow C_6H^-(j_1') + \text{o-; p-}H_2(j_2'), \quad (1)$$

and collisions with helium described by

$$C_6H^-(j_1) + He \rightarrow C_6H^-(j_1') + He, \quad (2)$$

where j_1 and j_2 are the rotational levels of C_6H^- and H_2, respectively. Rotational energy levels of C_6H^- are presented in Table 1 and were calculated from the rotational constants of McCarthy et al. (2006): $B_e = 0.045\,927$ cm^{-1}, $\alpha_e = 3.3356 \times 10^{-5}$ cm^{-1} and $D_e = 1.079 \times 10^{-9}$ cm^{-1}. The small values yield closely spaced rotational levels, and therefore high-j levels are significantly populated at a low temperature so that one has to provide data for a large number of rotational levels. In addition, the large well depths seen in the PESs

Table 2. Harmonic frequencies of C_6H^-.

Level	Frequency (cm^{-1})
1	82.89
2	82.89
3	210.61
4	210.61
5	340.65
6	340.65
7	429.94
8	429.94
9	486.62
10	486.62
11	618.10
12	1164.03
13	1933.71
14	2096.29
15	2177.11
16	3468.60

(−712.1 and −68.8 cm^{-1} for the C_6H^-–H_2 and C_6H^-–He systems, respectively) imply that large basis sets are needed for convergence.

The scattering calculations were performed on the recent four-dimensional (4D) C_6H^-–H_2 and two-dimensional (2D) C_6H^-–He PESs in their respective ground electronic states (Walker et al. 2016). Both potentials were constructed from high-level *ab initio* calculations computed at the explicitly correlated coupled cluster with the single, double and scaled perturbative triple excitations [CCSD(T*)-F12b/VTZ-F12] level of theory. The resulting interpolative PESs have wavenumber accuracy. Both molecules were treated as rigid rotors; the H_2 fragment used the vibrationally averaged bond distance for para-hydrogen, while C_6H^- was optimized at the CCSD(T*)-F12b/VTZ-F12 level. To probe the validity of the rigid rotor approximation for C_6H^-, harmonic frequencies were calculated at the CCSD(T)-F12b/VDZ-F12 level and are given in Table 2. There are five pairs of degenerate bends, followed by six stretches that maintain collinearity. The lowest bending mode is 40 cm^{-1} above the highest rotational state considered in this work ($j_1 = 30$). Hence, we expect a moderate impact of the vibrational channels on the pure rotational excitation. All rotational calculations were carried out in the ground vibrational manifold. While recent work on the He–C_3 system shows that the rigid monomer approximation may produce inaccurate cross-sections for collision energies above the first excited bending level (Stoecklin, Denis-Alpizar & Halvick 2015), the rotational–vibrational coupling in C_6H^- collisions is expected to be lower than that of C_3 due to the closely spaced rotational levels. The lowest harmonic frequencies represent the floppy structure of the entire molecule, not just a bending of the lone hydrogen atom. Therefore, our results are more similar to those of the He–HCN system, where the bending motion does not significantly affect pure rotational cross-sections (Stoecklin et al. 2013).

The 4D interaction potential with H_2 was expressed in Jacobi coordinates $V(\boldsymbol{R},\theta_1,\theta_2,\phi)$, where R is the distance from the C_6H^- centre of mass to the H_2 centre of mass, θ_1 is the angle between vector $\boldsymbol{R}$ and the C_6H^- bond axis, θ_2 is the angle between vector $\boldsymbol{R}$ and the H_2 bond axis and ϕ is the torsion angle between the two molecules, as shown in Fig. 1(a). The 2D C_6H^-–He PES was expressed as $V(R,\theta)$ using the Jacobi coordinates R, the distance from the C_6H^- centre of mass to the helium atom, and θ, the angle between $\boldsymbol{R}$ and the C_6H^- bond axis (see Fig. 1b).

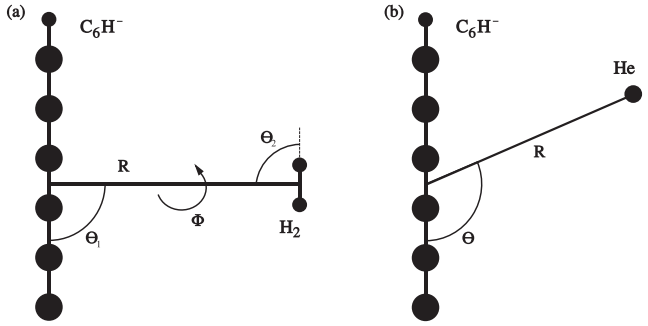

Figure 1. The Jacobi coordinates for (a) the 4D C_6H^-–H_2 and (b) the 2D C_6H^-–He PESs.

Computation of the collisional cross-sections was performed using the quantum non-reactive scattering code MOLSCAT (Hutson & Green 1994). The calculations spanned the energy range of 0.01–500 cm^{-1} in order to produce rate coefficients between 2 and 100 K. The fully quantal CC approach of Green (1975) was used to compute state-to-state cross-sections for rotational levels up to and including $j_1 = 10$ for all three colliders. For $11 < j_1 < 30$, the CS approximation (McGuire & Kouri 1974) was utilized in collisions of C_6H^- with para- and ortho-H_2 since the number of channels became prohibitively expensive. While the CS approximation is valid at high energies for repulsive interactions, it is expected to be less accurate (by ∼20–30 per cent) for low energies ($E_K < 50$ cm^{-1}) and with increasing j_1.

Special care had to be taken in the expansion of the interaction potentials. The PESs are largely anisotropic in two ways: (1) as the H_2 fragment approaches the ends or side of the long C_6H^- molecule; and (2) when the orientation of the H_2 fragment is either completely collinear or has a T-shaped approach to the larger molecule. Therefore, a large number of terms were necessary when expanding the interaction potential into radial and angular components. For C_6H^-–H_2, the PES was expanded as

$$V(R,\theta_1,\theta_2,\phi) = \sum_{l_1,l_2,l} v_{l_1,l_2,l}(R) A_{l_1,l_2,l}(\theta_1,\theta_2,\phi), \quad (3)$$

where $A_{l_1,l_2,l}$ are contracted normalized spherical harmonics. The angular dependence was expanded up to order $l_{1,\max} = 50$ for C_6H^-, while H_2 was expanded according to Legendre polynomials of order $l_{2,\max} = 4$. Likewise, the C_6H^-–He PES was expanded as

$$V(R,\theta) = \sum_{l_1=0}^{l_{1\max}} v_{l_1}(R) P_{l_1}(\cos\theta), \quad (4)$$

where P_{l_1} are the Legendre polynomials. Radial coefficients up to order $l_1 = 50$ were considered in the expansion. The reduced masses of the C_6H^-–H_2 and C_6H^-–He systems are $\mu = 1.961\,49$ and 3.794 57 uma, respectively.

The modified log-derivative Airy propagator of Alexander & Manolopoulos (1987) with a variable step size was used to solve the coupled-channel equations from $R = 4$ to $100a_0$ at low energies, with a progressive decrease in maximum propagation to $R = 40a_0$ at the highest energies. The rotational basis set for the calculations included all open channels and several closed channels to secure the convergence of the largest cross-sections within 10 per cent. Therefore, for the highest energy considered, the basis set extended up to $j_1 = 40$.

The rotational basis for the collider H_2 included only the ground para-H_2($j_2 = 0$) and ortho-H_2($j_2 = 1$) levels. The additional inclusion of either the $j_2 = 2$ or the $j_2 = 3$ levels in the para-H_2 and ortho-H_2 bases, respectively, led to cross-sections that were within 10 per cent of the values calculated with only the $j_2 = 0$ and $j_2 = 1$ levels. Table 3 displays the convergence of several $C_6H^-(j_1 \rightarrow j_1')$ transitions at a total energy of 100 cm^{-1} as a function of the rotational basis sets [expressed as $(j_1^{\max}, j_2^{\max})$] for collisions with para-H_2. The large computational expense resulting from the addition of higher H_2 rotational levels in the basis set was therefore eliminated without a significant effect on the cross-sections.

Table 3. Convergence of the rotational bases at $E = 100$ cm^{-1}.

Transition $j_1 \rightarrow j_1'$	(40,0)[a]	(40,2)	(45,0)	(50,0)
1 → 0	18.89[b]	18.93	18.56	18.30
2 → 0	7.55	8.25	7.56	7.45
2 → 1	28.99	28.64	29.84	29.48
5 → 4	36.96	35.30	37.30	36.54
10 → 5	7.45	6.49	7.67	7.56
10 → 9	38.88	37.73	38.47	39.20
20 → 10	2.94	3.41	3.00	2.88
20 → 19	39.74	41.29	39.71	40.18

Notes. [a]Rotational bases are expressed as $(j_1^{\max}, j_2^{\max})$.
[b]Cross-section ($\times 10^{-16}$ cm^2).

Table 4. Comparison of CC and CS cross-sections ($\times 10^{-16}$ cm^2) for collisions of C_6H^- with para-H_2.

Transition	10 cm^{-1}		50 cm^{-1}		100 cm^{-1}	
$j_1 \rightarrow j_1'$	CC	CS	CC	CS	CC	CS
1 → 0	34.83	25.92	19.61	18.70	14.49	18.89
2 → 0	9.74	8.72	7.76	6.16	5.57	7.55
2 → 1	52.87	41.25	28.60	27.30	24.80	28.99
3 → 0	5.73	8.99	2.77	4.42	3.97	4.28
3 → 1	21.02	18.99	12.89	11.88	12.52	11.97
3 → 2	61.07	54.13	33.18	30.89	28.90	34.27
5 → 0	4.42	3.83	1.72	2.76	1.82	2.05
5 → 1	13.25	12.55	3.97	7.12	5.91	3.14
5 → 2	23.94	27.02	9.57	11.36	10.73	10.79
5 → 3	41.18	31.07	17.67	16.29	18.05	15.11
5 → 4	78.93	63.00	39.14	33.05	32.43	36.96
10 → 0	3.84	2.99	0.86	0.57	0.62	0.18
10 → 1	10.70	4.88	2.58	2.21	1.78	1.26
10 → 2	19.24	18.19	4.15	2.98	3.33	1.19
10 → 3	25.29	11.48	6.34	5.39	4.44	3.53
10 → 4	30.53	30.82	7.17	6.18	6.81	3.13
10 → 5	38.23	22.08	9.77	9.53	8.37	7.45
10 → 6	44.32	37.59	10.86	10.43	12.26	5.54
10 → 7	53.76	52.28	14.67	15.80	15.71	14.57
10 → 8	67.63	69.08	25.35	18.91	22.80	17.48
10 → 9	104.93	107.37	41.39	37.61	41.71	38.88

A comparison between the full CC integral cross-sections and those obtained via the CS approximation is shown for collisions of C_6H^- with para-H_2 in Table 4. For the low total energy of 10 cm^{-1}, the difference between the two methods is typically of the order of ∼10–50 per cent, with a better agreement between the even-Δj_1 transitions (∼10 per cent). The CC and CS methods agree better at the higher energy of 50 cm^{-1} and even more so at 100 cm^{-1}, where the techniques produce cross-sections that are, on average, within ∼10–30 per cent of one another. In contrast, though, the odd-Δj_1 transitions at high energies have a better agreement (∼10 per cent) than the even-Δj_1 transitions (∼20–30 per cent). The similarity between the CC and CS rate coefficients illustrates the accuracy

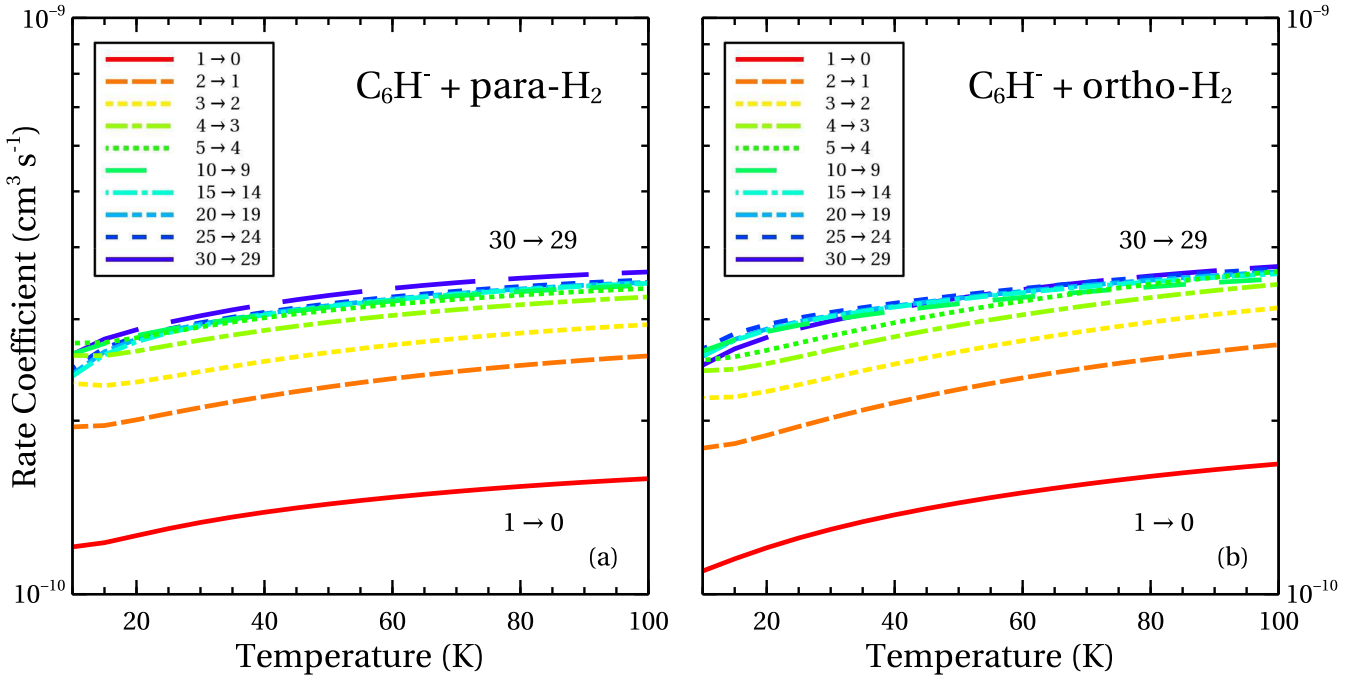

Figure 2. Rate coefficients for collisions of C_6H^- with (a) para-H_2 and (b) ortho-H_2. Both are remarkably similar in magnitude.

of the CS approximation that is well adapted to scattering between heavy particles.

The state-to-state collisional rate coefficients for a transition from initial rotational state j to final rotational state j' at a given temperature, $k_{j\to j'}(T)$, were obtained by averaging the respective cross-section, $\sigma_{j\to j'}(E_j)$, over a Boltzmann distribution of collision energies,

$$k_{j\to j'}(T) = \left(\frac{8k_BT}{\pi\mu}\right)^{1/2} \frac{1}{(k_BT)^2} \times \int_0^\infty \sigma_{j\to j'}(E_j)\exp(-E_j/k_BT)E_j\,dE_j, \quad (5)$$

where k_B is the Boltzmann constant. While de-excitation state-to-state rate coefficients are reported here, rate coefficients for the reverse transitions can be obtained via a detailed balance according to

$$k_{j'\to j}(T) = \frac{2j+1}{2j'+1}\exp\left(\frac{\epsilon_{j'}-\epsilon_j}{k_BT}\right)k_{j\to j'}(T), \quad (6)$$

where ϵ_i indicates the energy of the ith rotational level.

3 RESULTS

3.1 Rate coefficients

State-to-state inelastic rate coefficients for temperatures from 10 to 100 K for collisions of C_6H^- with para- and ortho-H_2 are shown in Fig. 2. These low-lying and selected $\Delta j_1 = -1$ transitions exhibit fairly constant values throughout the temperature range, of the order of a few $\sim 10^{-10}$ cm^3 s^{-1}, and increase only slightly with an increasing temperature. Remarkably, there is no significant difference of magnitude in the state-to-state rate coefficients for para- and ortho-H_2. This is quite different from neutral species that typically show an enhancement in ortho-H_2 collisions when compared to para-H_2 (e.g. Roueff & Lique 2013).

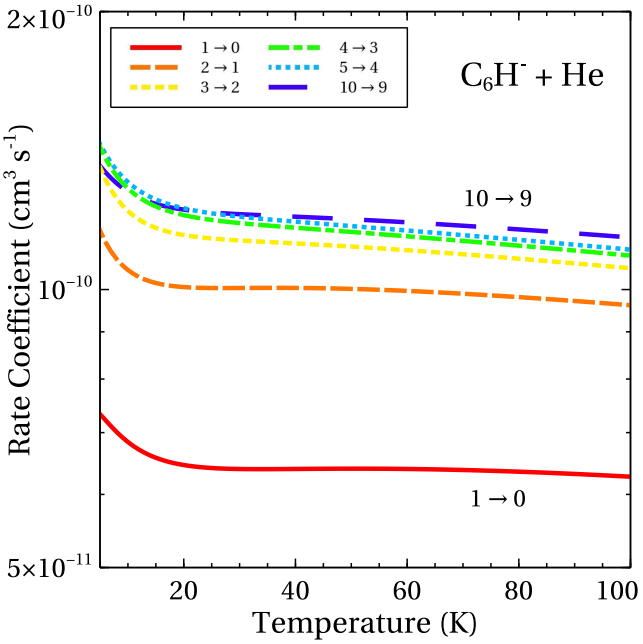

Figure 3. Rate coefficients for collisions of C_6H^- with He using the CC method.

The rate coefficients for collisions of C_6H^- with helium for $\Delta j_1 = -1$ transitions are shown in Fig. 3. These rate coefficients display exceptionally flat behaviour like those of H_2 along the 10–100 K temperature range. However, the magnitudes of the state-to-state transitions are typically of the order of ∼2–3 less than the rate coefficients for H_2 collisions.

The propensity rules for these pure rotational transitions are also interesting to inspect. Fig. 4 shows the de-excitation rate coefficients for transitions out of $j_1 = 10$ for collisions with para-H_2, ortho-H_2 and He at $T = 10$ K, while Fig. 5 shows the same transitions for

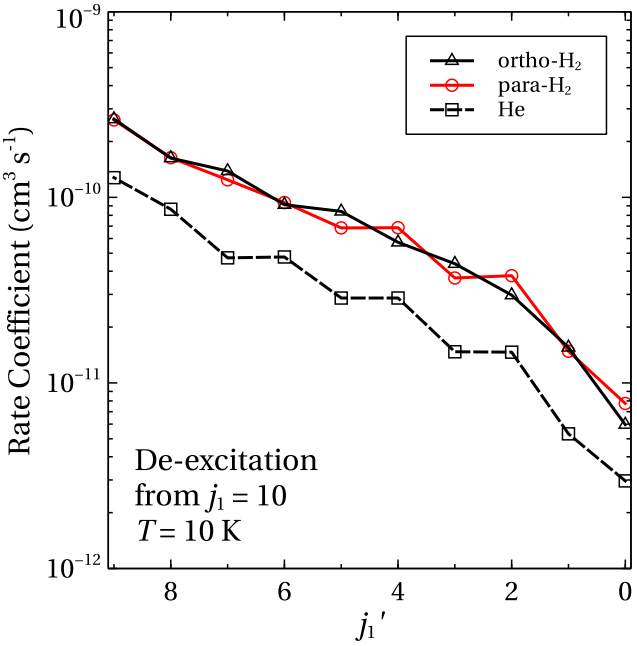

Figure 4. Propensity rules for transitions out of initial $j_1 = 10$ for collisions of C_6H^- with H_2 and He at $T = 10$ K.

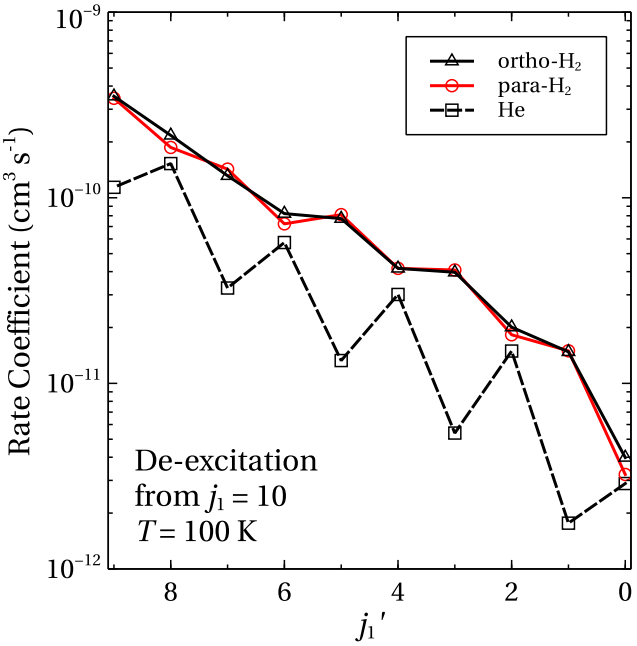

Figure 5. Propensity rules for transitions out of initial $j_1 = 10$ for collisions of C_6H^- with H_2 and He at $T = 100$ K.

$T = 100$ K. The $\Delta j_1 = -1$ transition is dominant for both para- and ortho-H_2 at all temperatures. However, in collisions with helium, the $\Delta j_1 = -1$ transition is dominant at a low temperature, whereas the $\Delta j_1 = -2$ transition dominates at a high temperature. The propensity rules are not consistent – this is also exhibited in $\Delta j_1 = -3$ and -4, which are of similar magnitude at 10 K, while $\Delta j_1 = -4$ clearly dominates $\Delta j_1 = -3$ at 100 K.

The similarity of the magnitudes and propensity rules for the para- and ortho-H_2 collisional rate coefficients shows that effects in the long-range interaction outweigh those from the short range in anionic scattering. The C_6H^-–H_2 system has a large well depth

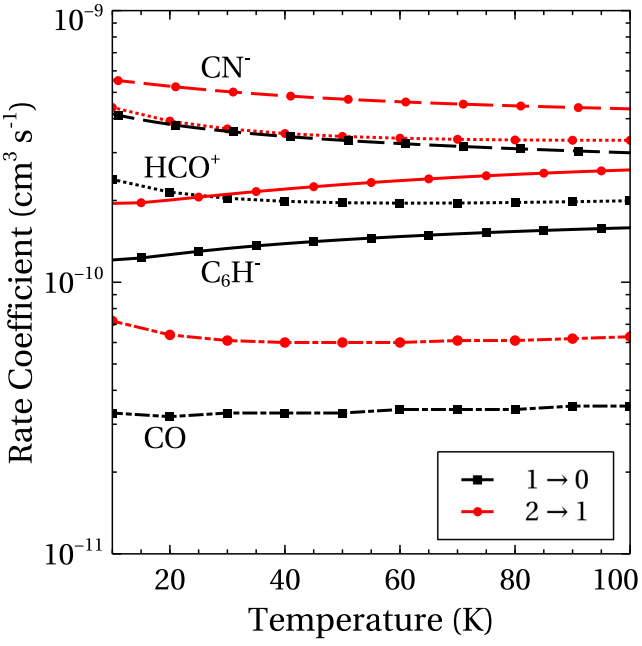

Figure 6. A comparison of the rate coefficients for the first two $\Delta j = -1$ transitions in collisions between para-H_2 and CO (dash–dotted), C_6H^- (solid), CN^- (dashed) and HCO^+ (dotted) for $10 \leq T \leq 100$ K.

of -712.1 cm^{-1}, and in the short range, the orientation of the H_2 fragment is effectively averaged. At a large interaction distance, the effects from the H_2 para- and ortho-moieties are less established, and similar rate coefficients are obtained. A likewise similarity of the para- and ortho-H_2 rate coefficients is also seen in collisions with CN^- (Kłos & Lique 2011).

The deep well of the C_6H^-–H_2 PES also gives rise to comparatively high rate coefficients. While known rate coefficients have been used to estimate unknown rate coefficients, the large well depths of anionic systems cause predictions from neutral molecules to be poor. For example, C_6H^- and CO both have a $^1\Sigma$ ground state, but the neutral CO–H_2 system has a significantly shallower well of -85.9 cm^{-1} (Yang et al. 2015) compared to the well depth of C_6H^-. Likewise, the CN^-–H_2 system also has a large well of -875.4 cm^{-1} (Kłos & Lique 2011), which significantly increases the magnitude of its rate coefficients. De-excitation rate coefficients between the first two transitions of CO, C_6H^- and CN^- in collisions with para-H_2 are shown in Fig. 6, and we can see that those of the anionic species are significantly larger in magnitude than those of the neutral molecule. The rate coefficients for CN^- are an order of magnitude larger than CO, while the rate coefficients for C_6H^- are larger than those of CO by a factor of 2 to 3. Rate coefficients for collisions of H_2 with the cation HCO^+ from Yazidi, Ben Abdallah & Lique (2014) are also shown in comparison to the anions in Fig. 6. The rate coefficients for this cation are similar to the anions, with values of the order of a few $\sim 10^{-10}$ cm^3 s^{-1}, higher than those of CO. The depth of the well causes the magnitude of ionic rate coefficients to be larger.

While the rate coefficients with helium as a collider were much less computationally expensive than those of H_2, molecular hydrogen is the primary collider in the cold, dense environments where C_6H^- is detected. Unfortunately, a simple estimate of H_2 rate coefficients from those of He is not straightforward (see e.g. Walker et al. 2014). Since the variance of the state-to-state rate coefficients across this energy range is primarily flat, an estimate of H_2 rate

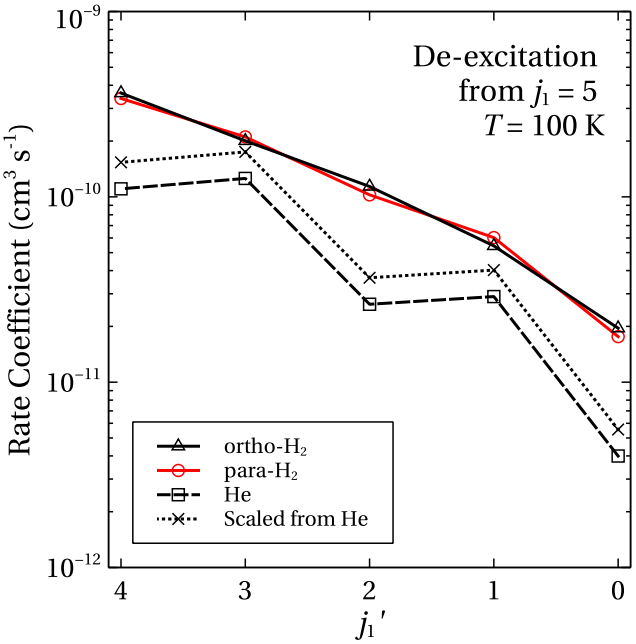

Figure 7. Propensity rules for transitions out of initial $j_1 = 5$ at $T = 100$ K for collisions of C_6H^- with H_2, with He, and scaled using the helium rate coefficients multiplied by 1.39.

coefficients from those of He via the typical reduced-mass scaling approach may seem plausible. This approach scales the helium collisional rates to those of H_2 by multiplying the He rates by the square root of the ratio of reduced masses, i.e. $k_{H_2} = (\mu_{He}/\mu_{H_2})^{(1/2)} k_{He}$, which, in our case, equals 1.39. The rates produced this way, however, mimic the propensity rules for helium collisions, which are quite different from those of H_2, as shown in Fig. 7 for de-excitation out of initial level $j_1 = 5$. While there is almost an agreement for the even Δj_1-scaled transitions for this particular temperature, the odd transitions based on this scaling approach are not accurate, and unfortunately the odd $\Delta j_1 = -1$ transitions are exactly those that are detected in IRC +10216 and TMC-1. Regrettably, the rate coefficients for collisions with para- or ortho-H_2 cannot simply be estimated using this standard reduced-mass scaling approach.

3.2 Astrophysical application

Finally, we use these new rate coefficients to obtain critical densities for C_6H^-. When collisional processes dominate in astrophysical environments, the LTE approximation is often used to obtain the quantum level populations of a given molecule. Contributions from radiative transitions are neglected, and a Boltzmann distribution is assumed for the level populations. However, for many regions in the ISM, such as in molecular clouds and other low-temperature regions where anions are detected, the inclusion of radiative transitions is important and cannot be neglected.

We define the critical density $n_{crit}(i)$ for any quantum level i, where the effects from collisional and radiative transitions bear equal weight as

$$n_{crit}(i) = \frac{\sum_{j<i} A_{ij}}{\sum_{j\neq i} k_{ij}}, \quad (7)$$

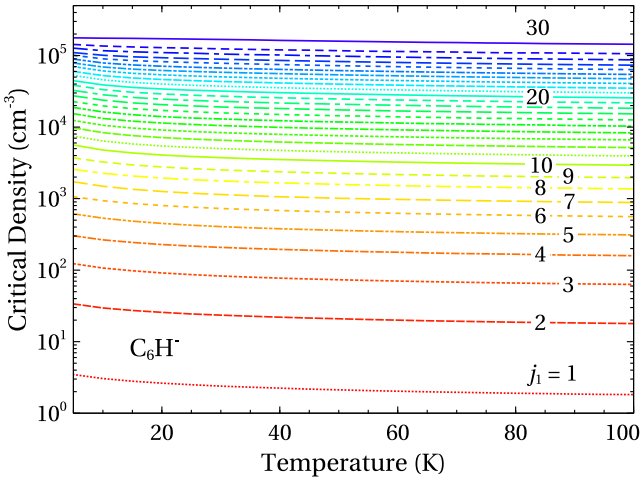

Figure 8. Critical densities for rotational levels of C_6H^- up to $j_1 = 30$.

where A_{ij} is Einstein's spontaneous emission probability (A-value) from level i to level j and k_{ij} is the rate coefficient for collisional excitation or de-excitation out of level i.

Using the rate coefficients from Section 3.1 and A-values from M. Agundez (private communication), who adopted a dipole moment of 8.2 Debye from Blanksby et al. (2001), the critical densities for C_6H^- were calculated and are shown in Fig. 8. For low-density environments that only have a few particles per cubic centimetre, the critical density of the lowest excited level is surpassed, and in fact, in these regions, the first few rotational levels are in LTE. For higher rotational levels, the critical density increases and at $j_1 = 30$ becomes $\sim 10^5$ cm^{-3}, which is typically the density in circumstellar gas and star-forming regions. Therefore, in low- to moderate-density environments, high rotational levels can radiatively de-excite before they undergo collisional de-excitation, and to accurately obtain the level populations and model anionic line emission, the rate coefficients calculated in this work are required. Although using LTE may be a good approximation in TMC-1, in star-forming regions that are at a temperature of 40–50 K, the high-j_1 levels will be out of equilibrium and the collisional rates presented here are needed for modelling C_6H^- emission.

4 SUMMARY AND DISCUSSION

Fundamental molecular data are required to produce accurate models of anions in astrophysical environments such as circumstellar envelopes and star-forming regions. Since molecular level populations are often out of equilibrium in these regions, collisional rate coefficients with the dominant species are required. To form a more complete set of rate coefficients, dynamics calculations of the C_6H^- molecule in collisions with para-H_2, ortho-H_2 and He were presented here. The high level of theory in the *ab initio* calculations of Walker et al. (2016) resulted in new, accurate 4D and 2D PESs for the C_6H^-–H_2 and C_6H^-–He systems, respectively, upon which dynamics calculations were carried out. The CC method was employed in scattering calculations for the first 11 rotational levels of C_6H^-, while the CS approximation was used to calculate its rotational excitation in collisions with para- and ortho-H_2 up to $j_1 = 30$. The CC and CS calculations agree relatively well, especially at higher collisional energies where the CS approximation becomes increasingly valid.

The resulting state-to-state rate coefficients range in temperature from 2 to 100 K and will be made available in the LAMBDA

(Schöier et al. 2005) and BASECOL (Dubernet et al. 2013) data bases. While both para- and ortho-H_2 have dominant $\Delta j_1 = -1$ rate coefficients for all temperatures, the propensity rules for helium collisions change with temperature. At low temperatures, the rate coefficients for the $\Delta j_1 = -1$ transitions are dominant, while at high temperatures, the $\Delta j_1 = -2$ transitions dominate. The magnitudes of the rate coefficients for C_6H^- are similar to those of CN^-, greater than those of CO. These calculations also demonstrated the inaccuracy of standard reduced-mass scaling. Finally, critical densities for the rotational levels of C_6H^- were computed, and although the LTE approximation may be valid for the first few levels in star-forming regions, the upper levels would have non-thermal populations. Since the most accurate PESs have been used to perform the scattering calculations, and the largest rate coefficients for both the C_6H^-–H_2 and C_6H^-–He systems are converged to within 10 per cent, it is expected that the results are accurate to within an order of magnitude, and most likely within a factor of 2 to 3. The resulting inelastic rate coefficients for collisions of C_6H^- with H_2 and He will aid in constraining astrophysical anion chemistry and help to accurately model regions containing anions such as IRC +10216.

ACKNOWLEDGEMENTS

This research was supported by the French National Research Agency (ANR) through a grant to the Anion Cos Chem project (ANR-14-CE33-0013), the Centre National de la Recherche Scientique-Institut National des Sciences de l'Univers (CNRS-INSU) Programme National de Physique et Chimie du Milieu Interstellaire and the National Science Foundation (CHE-1300945 to RD). This work was granted access to the High Performance Computing (HPC) resources of Institut du Developpement et des Ressources en Informatique Scientique (IDRIS) under the Allocation No. 2016-047659 made by GENCI (Grand Equipement National de Calcul Intensif).

REFERENCES

Agúndez M. et al., 2010, A&A, 517, L2
Alexander M. H., Manolopoulos D. E., 1987, J. Chem. Phys., 86, 2044
Blanksby S. J., McAnoy A. M., Dua S., Bowie J. H., 2001, MNRAS, 328, 89
Brünken S., Gupta H., Gottlieb C. A., McCarthy M. C., Thaddeus P., 2007, ApJ, 664, L43
Cernicharo J., Guélin M., Agúndez M., Kawaguchi K., McCarthy M., Thaddeus P., 2007, A&A, 467, L37
Cernicharo J., Guélin M., Agúndez M., McCarthy M. C., Thaddeus P., 2008, ApJ, 688, L83
Dalgarno A., McCray R. A., 1973, ApJ, 181, 95
Dubernet M.-L. et al., 2013, A&A, 553, A50
Green S., 1975, J. Chem. Phys., 62, 2271
Gupta H., Gottlieb C. A., McCarthy M. C., Thaddeus P., 2009, ApJ, 691, 1494
Herbst E., 1981, Nature, 289, 656
Hutson J. M., Green S., 1994, Distributed by Collaborative Computational Project No. 6. Engin., Phys. Sci. Res. Council, Swindon
Kłos J., Lique F., 2011, MNRAS, 418, 271
McCarthy M. C., Gottlieb C. A., Gupta H., Thaddeus P., 2006, ApJ, 652, L141
McGuire P., Kouri D. J., 1974, J. Chem. Phys., 60, 2488
Roueff E., Lique F., 2013, Chem. Rev., 113, 8906
Sakai N., Sakai T., Osamura Y., Yamamoto S., 2007, ApJ, 667, L65
Schöier F. L., van der Tak F. F. S., van Dishoeck E. F., Black J. H., 2005, A&A, 432, 369
Stoecklin T., Denis-Alpizar O., Halvick P., Dubernet M.-L., 2013, J. Chem. Phys., 139, 124317
Stoecklin T., Denis-Alpizar O., Halvick P., 2015, MNRAS, 449, 3420
Thaddeus P., Gottlieb C. A., Gupta H., Brünken S., McCarthy M. C., Agúndez M., Guélin M., Cernicharo J., 2008, ApJ, 677, 1132
Walker K. M., Yang B. H., Stancil P. C., Balakrishnan N., Forrey R. C., 2014, ApJ, 790, 96
Walker K. M., Dumouchel F., Lique F., Dawes R., 2016, J. Chem. Phys., 145, 024314
Yang B., Zhang P., Wang X., Stancil P. C., Bowman J. M., Balakrishnan N., Forrey R. C., 2015, Nat. Comm., 6, 6629
Yazidi O., Ben Abdallah D., Lique F., 2014, MNRAS, 441, 664

This paper has been typeset from a TEX/LATEX file prepared by the author.